Chapter 2
Time

2.1 Stability of Oscillators

In the following it will be of relevance to have a good idea about the quality of an atomic clock (oscillator). One quality criterion is the stability of the oscillator, determined by the stochastic fluctuations in frequency space about the norm frequency. Usually the stability of an oscillator is characterized by the so-called *2-point Allan variance* (named after the American physicist David W. Allan; Allan et al. 1988) that will be discussed now.

Every precise frequency generator like a quartz oscillator or an atomic frequency standard shows frequency fluctuations both of random as well as systematic character. Systematic fluctuations are, e.g.,

- Frequency drifts, e.g., in quartz oscillators caused by aging (by the forming of dislocations in the lattice)
- Frequency modulations caused by the low-frequency part of the supply current or
- Quasiperiodic frequency modulations resulting from temperature and pressure variations

Sporadically in such oscillators, also unexplained frequency jumps might occur.

For the following considerations let t be the (Newtonian) time variable. Let us describe the output signal (e.g., alternating current) of an ideal oscillator by

$$U(t) = U_0 \sin 2\pi f_0 t,$$

where U_0 (f_0) is some norm amplitude (frequency). Every realistic, nonideal oscillator will show time-dependent amplitude and phase fluctuations, i.e.,

$$U(t) = [U_0 + \epsilon(t)] \times \sin [2\pi f_0 t + \varphi(t)] .$$

M. Soffel and R. Langhans, *Space-Time Reference Systems*, Astronomy and Astrophysics Library, DOI 10.1007/978-3-642-30226-8_2, © Springer-Verlag Berlin Heidelberg 2013

For the problem of time determination, amplitude variations $\epsilon(t)$ basically play no role, so we write

$$U(t) = U_0 \sin \phi(t) \tag{2.1}$$

with

$$\phi(t) = 2\pi f_0 t + \varphi(t). \tag{2.2}$$

With the actual frequency

$$f(t) = f_0 + \frac{1}{2\pi}\frac{\mathrm{d}\varphi(t)}{\mathrm{d}t}$$

we can define the frequency fluctuation as

$$\Delta f(t) \equiv f(t) - f_0 = \frac{1}{2\pi}\frac{\mathrm{d}\varphi(t)}{\mathrm{d}t}.$$

With the relative frequency fluctuation

$$y(t) \equiv \frac{\Delta f(t)}{f_0} \tag{2.3}$$

we can define the phase time $x(t)$ as

$$x(t) \equiv \int_{t_0}^{t} y(t)\mathrm{d}t. \tag{2.4}$$

The value of $x(t)$ corresponds to the error in time, a clock shows at time t since the start at t_0. The relative frequency fluctuation $y(t)$ cannot be measured directly. Only a mean value taken over a time interval τ is measurable:

$$y(t_k, \tau) = \frac{1}{\tau}\int_{t_k}^{t_k+\tau} y(t)\,\mathrm{d}t = \frac{1}{\tau}\left[x(t_k + \tau) - x(t_k)\right]. \tag{2.5}$$

The phase time $x(t)$ of some test oscillator can be measured by means of a reference oscillator. Simple conditions prevail if the frequency fluctuations of the reference oscillator can be neglected (Fig. 2.1). For the determination of the phase time an impulse counter is employed. If, e.g., the reference oscillator and the test oscillator both produce a well-defined impulse every second, then the phase time between the second pulses can be determined if a second pulse of the reference oscillator starts the counter at time t and the following second pulse of the test oscillator stops the counter. Then the counter reading determines the phase time $x(t)$.

Often, we encounter the situation that $y(t)$ can be written as

$$y(t) = y_r(t) + at + y_0\,,$$

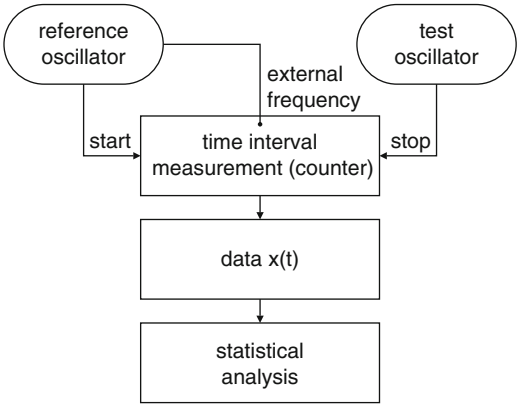

Fig. 2.1 Simple measuring assembly for the determination of the phase time $x(t)$

where $y_r(t)$ denotes a random fluctuation, a is the aging coefficient, and y_0 denotes a constant frequency shift. The resulting phase time $x(t)$ is then given by

$$x(t) = x_r(t) + \frac{1}{2}at^2 + y_0 t$$

with

$$x_r(t) = \int y_r(t)\,\mathrm{d}t + x_0\,.$$

Under standard conditions,

$$\int_{t_0}^{t} y_r(t)\,\mathrm{d}t = \int_{t_0}^{t} x_r(t)\,\mathrm{d}t = 0.$$

We will now define a *measuring series* $\mathcal{M}(N, \Delta t, \tau)$ for $y(t, \tau)$. In such a series N, different y_k values are obtained by averaging over time intervals of length τ in regular intervals of time $\Delta t = t_{k+1} - t_k$ (Fig. 2.2). From such a measuring series we can derive a mean value

$$<y_i>_N \equiv \frac{1}{N}\sum_{k=1}^{N} y_k \tag{2.6}$$

and the variance (Fig. 2.2)

$$\sigma_y^2(N, \Delta t, \tau) \equiv \frac{1}{N}\sum_{k=1}^{N}(y_k - <y_i>_N)^2. \tag{2.7}$$

To define a statistically meaningful quantity we could consider a very large number of individual measurements, $N \to \infty$. Another possibility is to repeat the measuring series $\mathcal{M}(N, \Delta t, \tau)$ very often (at convenient times). We will now assume that the

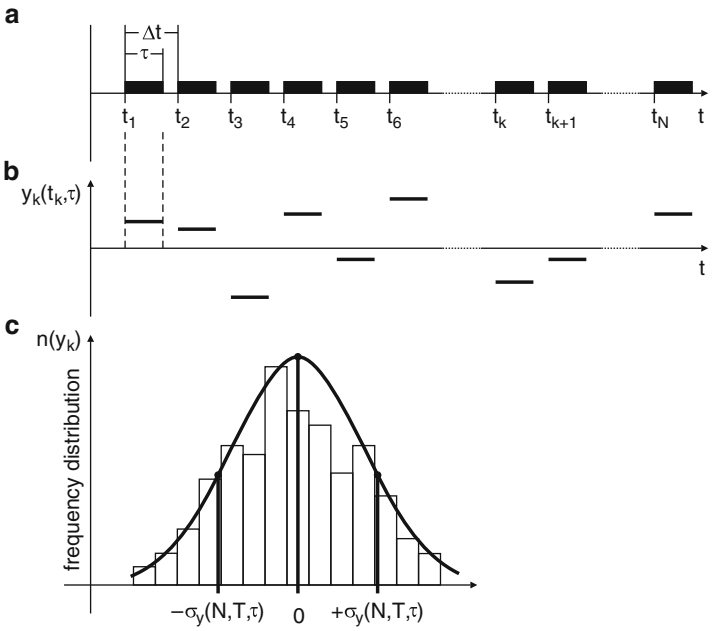

Fig. 2.2 (**a**) Measurement intervals for the determination of frequency fluctuations; (**b**) measurements averaged over the time interval τ; (**c**) frequency distribution of $y_k(t_k,\tau)$

measuring series is performed M times. As stability measure of the oscillator we can then define the Allan variance as

$$<\sigma_y^2(N,\Delta t,\tau)>\equiv \lim_{M\to\infty}\frac{1}{M}\sum\nolimits_{i=1}^{M}\sigma_{y_i}^2(N,\Delta t,\tau). \tag{2.8}$$

For the special case of $N=2$ we thereby get the 2-point Allan variance:

$$<\sigma_y^2(2,\Delta t,\tau)>\equiv \lim_{M\to\infty}\frac{1}{M}\sum\nolimits_{i=1}^{M}\sigma_{y_i}^2(2,\Delta t,\tau). \tag{2.9}$$

In that case

$$\begin{aligned}\sigma_{y_i}^2 &= \left[\left(y_{i,1}-\frac{y_{i,1}+y_{i,2}}{2}\right)^2+\left(y_{i,2}-\frac{y_{i,1}+y_{i,2}}{2}\right)^2\right]\\ &= \frac{1}{2}(y_{i,2}-y_{i,1})^2\end{aligned}$$

and, therefore,

$$<\sigma_y^2(2,\Delta t,\tau)>= \lim_{M\to\infty}\frac{1}{M}\sum\nolimits_{k=1}^{M}\frac{1}{2}(y_{k+1}-y_k)^2. \tag{2.10}$$

Let $F(f)$ be the Fourier transform of $y(t)$. Then, the spectral power density

$$S_y(f) = |F(f)|^2$$

is related with the autocovariance or autocorrelation function

$$C(\tau) = \int_{-\infty}^{+\infty} y(t)y(t+\tau)\,\mathrm{d}\tau \tag{2.11}$$

by

$$C(\tau) = \int_{-\infty}^{+\infty} \mathrm{e}^{2\pi \mathrm{i} f\tau}|F(f)|^2\,\mathrm{d}f \tag{2.12}$$

or

$$|F(f)|^2 = \int_{-\infty}^{+\infty} \mathrm{e}^{-2\pi \mathrm{i} f\tau}C(\tau)\,\mathrm{d}\tau, \tag{2.13}$$

according to the Wiener–Khinchin theorem.

In most cases the spectral power density $S_y(f)$ of an oscillator can be represented in the form

$$S_y(f) = h_{-2}f^{-2} + h_{-1}f^{-1} + h_0 + h_1 f + h_2 f^2 \tag{2.14}$$

and the various f^s-terms can be related with different kinds of noises:

- h_{-2}: random walk in frequency (y).
- h_{-1}: flicker noise in frequency (y), caused, e.g., by fluctuations in the power supply unit.
- h_0: white frequency noise corresponding to random walk in phase.
- h_1: flicker phase noise caused by certain electronic devices.
- h_2: white phase noise caused by additive noise in the electronics.

Schematically this noise behavior is depicted in Fig. 2.3.

For every oscillator the Allan variance depends crucially upon the averaging time τ. Figure 2.4 shows the typical behavior of the Allan variance of an atomic clock as a function of the averaging time τ.

2.2 Bias and Drift

Besides stochastic fluctuations an actual frequency standard shows additional effects that can be modeled to some degree. If f_0 denotes the nominal frequency of the oscillator, then often the approach

$$f(t) - f_0 = \Delta f + \dot{f}(t - t_0) + f_r(t) \tag{2.15}$$

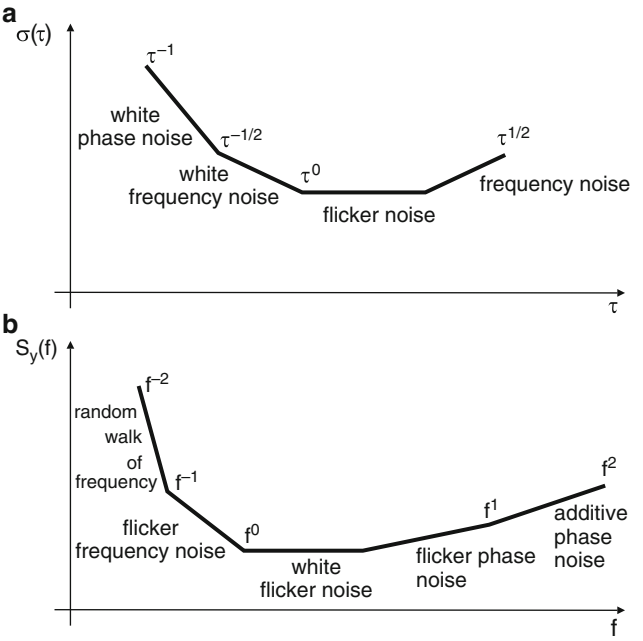

Fig. 2.3 Different kinds of noise in the time (panel **a**) and frequency (panel **b**) domain

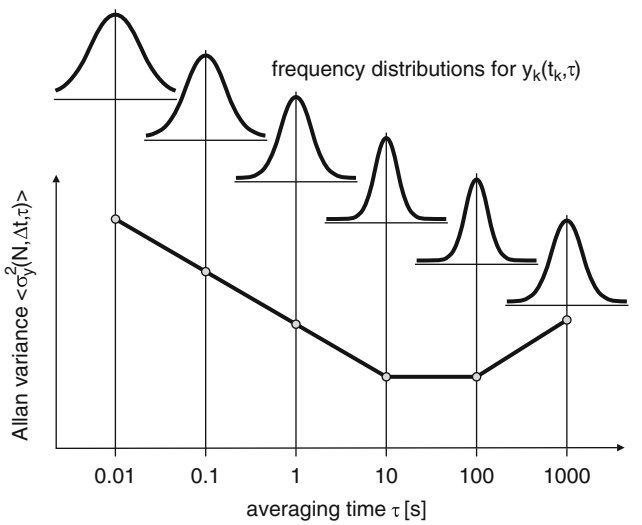

Fig. 2.4 Dependency of the Allan variance $<\sigma_y^2(N,\Delta t,\tau)>$ upon the averaging time τ for an atomic clock

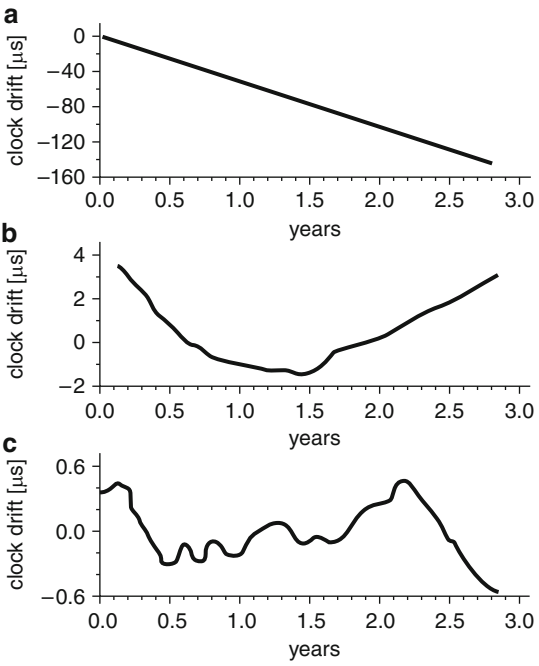

Fig. 2.5 Comparison of the behavior of a commercial Cs clock with those of an ensemble of atomic clocks. (**a**) Raw difference, (**b**) a linear trend was removed, (**c**) also a quadratic part was removed; from Jones and Tryon (1987). Copyright ©1987 Society for Industrial and Applied Mathematics. Reprinted with permission. All rights reserved

is sufficient. Here, Δf is called the bias, and the $\dot{f}$-term describes the drift of the oscillator; f_r describes the stochastic fluctuations.

Figure 2.5 shows a comparison of the behavior of a commercial Cs clock with those of the whole ensemble of atomic clocks from the US Naval Observatory (USNO; Washington). In the middle part a linear trend was removed; in the lower panel, also a quadratic part (Jones and Tryon 1987).

2.3 Quartz and Atomic Clocks

In a quartz oscillator one employs the mechanical vibrations of a quartz crystal showing the piezoelectrical effect: if the crystal is deformed, a voltage is induced. If on the other hand the crystal is placed between two electrodes and a voltage is applied, it will be deformed. If crystal vibrations are stimulated, they lead to a corresponding alternating current that can be used for the construction of a quartz clock. The clock frequency depends crucially upon shape and size of the crystal, and usually the electrodes are mounted directly on the quartz body.

Figure 2.6 schematically shows a typical block diagram of a quartz oscillator and Fig. 2.7 a typical variance behavior of commercial quartz oscillators.

In atomic oscillators certain atomic hyperfine levels in selected atoms, like hydrogen (^{1}H), rubidium (^{87}Rb), or cesium (^{133}Cs), are employed to significantly improve the stability of quartz oscillators. These hyperfine transitions result from

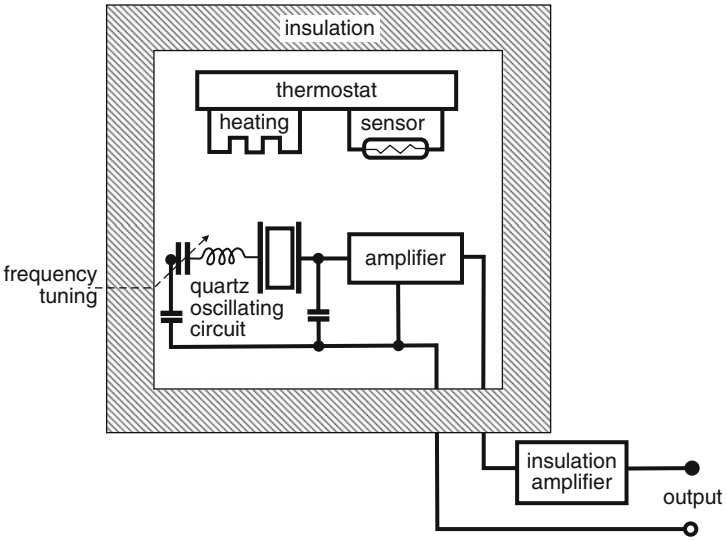

Fig. 2.6 Block diagram of a quartz oscillator

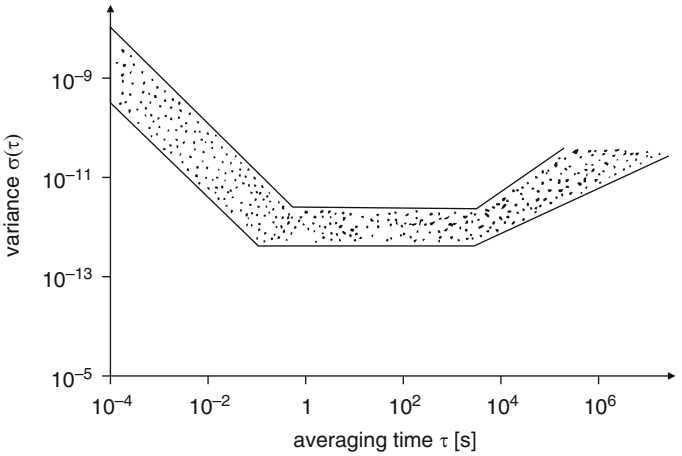

Fig. 2.7 Typical variance behavior of commercial quartz oscillators

the magnetic interaction between the spin of the atomic nucleus and the valence electron in the shell. The hyperfine transition frequencies lie in the microwave region where corresponding analysis techniques are available.

The hyperfine levels are characterized by a quantum number F describing the total spin of the atom. It results from the spin quantum number of the nucleus I and the valence electron with a value of $1/2$ (in units of the reduced Planck's constant $\hbar$):

$$F = I \pm \frac{1}{2}.$$

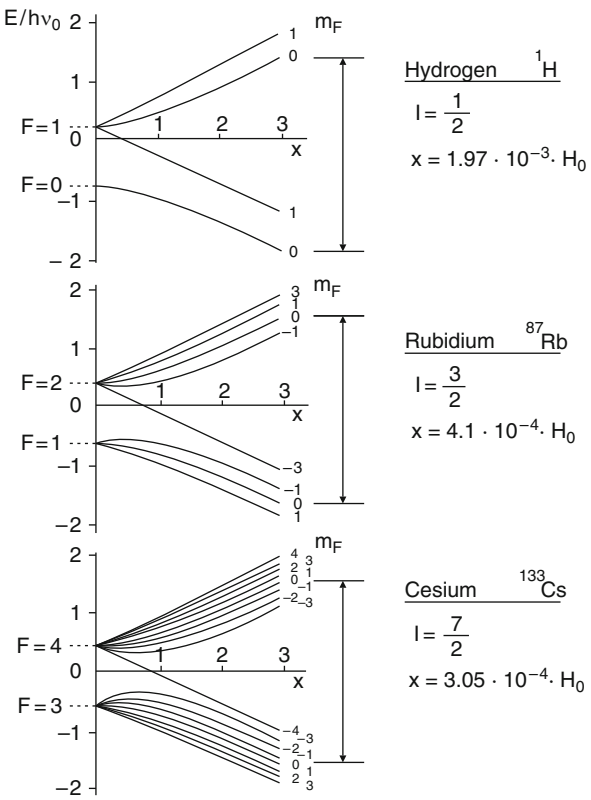

Fig. 2.8 Atomic hyperfine transitions are depicted that are employed in the construction of classical atomic clocks. The quantity x is a measure of the magnetic field strength

The two signs indicate that the direction of the electron's spin could be parallel or antiparallel to the spin of the nucleus.

From the values $I = 1/2$ (H), 3/2 (Rb), and 7/2 (Cs) correspondingly, one gets the following possibilities: ^{1}H: $F = 0$ and $F = 1$, ^{87}Rb: $F = 1$ and $F = 2$, ^{133}Cs: $F = 3$ and $F = 4$.

If a static magnetic field is applied, these levels are split into magnetic sublevels because of the Zeeman effect. These sublevels are further characterized by a magnetic quantum number m_F describing the component of the total spin in the direction of the applied magnetic field; it can take the values:

$$m_F = 0, \pm 1, \pm 2, \ldots, \pm F.$$

Thus, each F-level splits into $2F+1$ magnetic sublevels. Quantum mechanical rules allow only transitions with $\Delta F = 0, \pm 1$, and $\Delta m_F = 0, \pm 1$. For the realization of atomic frequency standards, transitions with $\Delta F = \pm 1, \Delta m_F = 0$ are best suited.

Atomic transitions in hydrogen, rubidium, and cesium standards are depicted in Fig. 2.8. Details of the fine and hyperfine splitting of the relevant energy levels in the cesium atom are shown in Fig. 2.9.

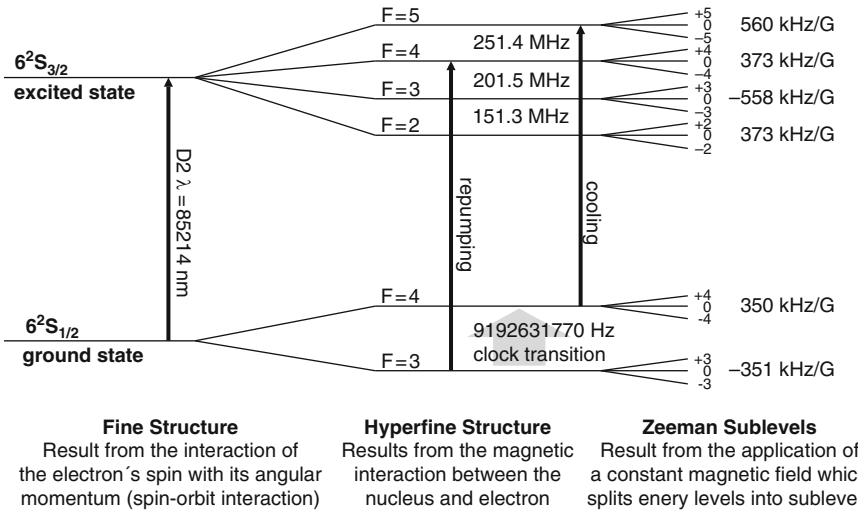

Fig. 2.9 The splitting of energy levels in the cesium atom. The fine structure splitting of spectral lines results from the spin–orbit coupling of the valence electron. The hyperfine splitting results from the interaction of the electron's spin with that of the atomic nucleus. A weak external magnetic field produces the Zeeman splitting

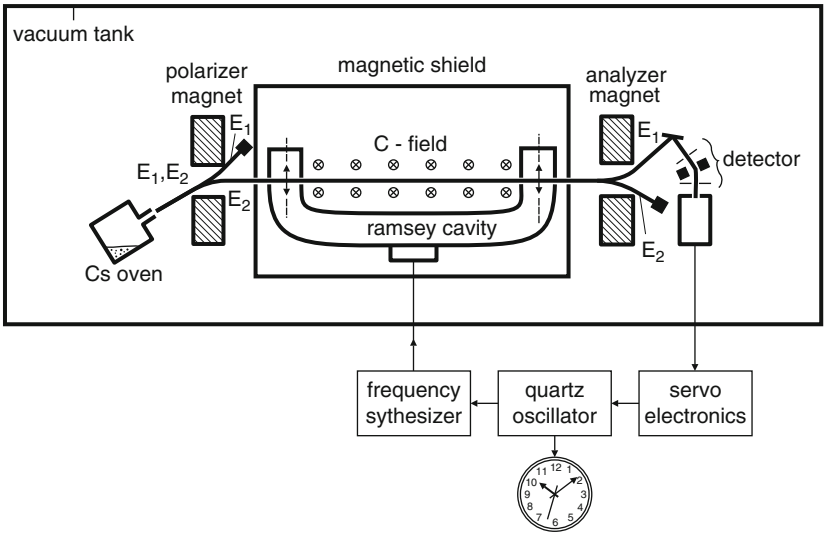

Fig. 2.10 Schematic diagram of a Cs frequency oscillator; from Riehle (2001). Courtesy of F. Riehle

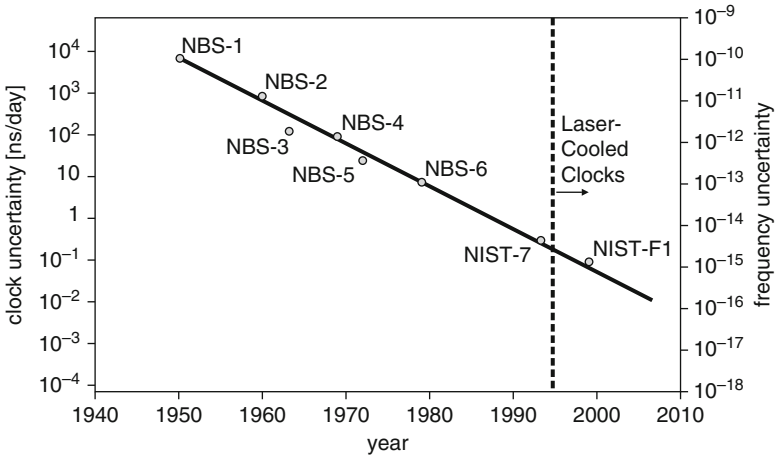

Fig. 2.11 Frequency stability of primary frequency standards at NIST, USA

2.4 Cesium Clocks

An atomic cesium clock is based upon the principle of atomic beam magnetic resonance as developed by I. Rabi before 1940. The essential parts of a cesium oscillator are shown in Fig. 2.10. A cesium oven at 100–200°C creates a cesium vapor that escapes through a small orifice. It enters an inhomogeneous magnetic field that splits the two energy levels of interest ($F = 3, F = 4$) due to their different magnetic dipole moments. Typically only the atoms in the upper ($F = 4$) level are allowed to enter the microwave resonator which is magnetically shielded, and the hyperfine splitting is achieved with a constant magnetic field. Inside the resonator, perpendicular to the beam axis (to reduce Doppler effects) a microwave signal derived from a quartz oscillator in the vicinity of the transition frequency of 9.2 GHz is applied. In case of resonance between this signal and the hyperfine levels in the cesium atom induced transitions will occur and the corresponding atoms having left the resonator will be deflected by a second magnet onto a particle detector. With a feedback loop the frequency of the quartz clock is steered until a maximal particle current is seen by the detector. In this way the stability of the quartz clock is improved significantly (Figs. 2.11 and 2.12).

2.5 Rubidium Clocks

Like the Cs generator the rubidium frequency oscillator is a passive system (Fig. 2.13). The clock transition of the ^{87}Rb isotope between the ($F = 2$) and ($F = 1$) state leads to a radiation at 6.835 GHz. Light from a Rb lamp, filtered

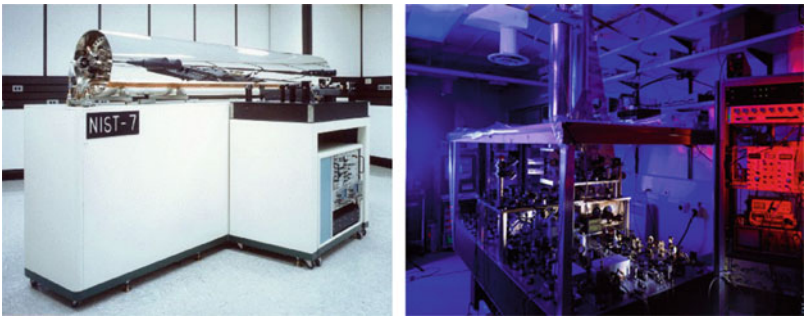

Fig. 2.12 The cesium standard NIST-7 (*left*) and the fountain clock NIST-F1 (*right*) with improved accuracy (NIST, USA)

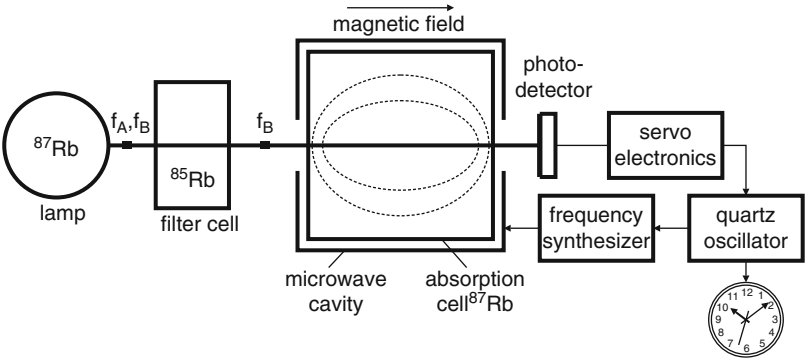

Fig. 2.13 Functional principle of a rubidium standard; from Riehle (2001). Courtesy of F. Riehle

by a ^{85}Rb gas cell by a mechanism called optical pumping, induces a different occupation of the two relevant energy levels in the rubidium gas inside a microwave resonator. The almost empty $F = 1$ level is again populated by the action of a high-frequency field derived from a quartz clock inducing $F = 2$ to $F = 1$ transitions. This leads again to an absorption of the pump signal. The corresponding change in transparency of the gas cell is monitored with a photo diode, and by means of a feedback loop, the stability of the quartz clock is improved. Frequency stabilities of commercial rubidium frequency standards are shown in Fig. 2.14.

2.6 H-Maser

Figure 2.15 shows schematically the principle of a hydrogen maser clock. In an H maser molecular hydrogen is dissociated, and the atoms in the upper clock level are forwarded into a storage bulb. This bulb, usually made from quartz glass, is

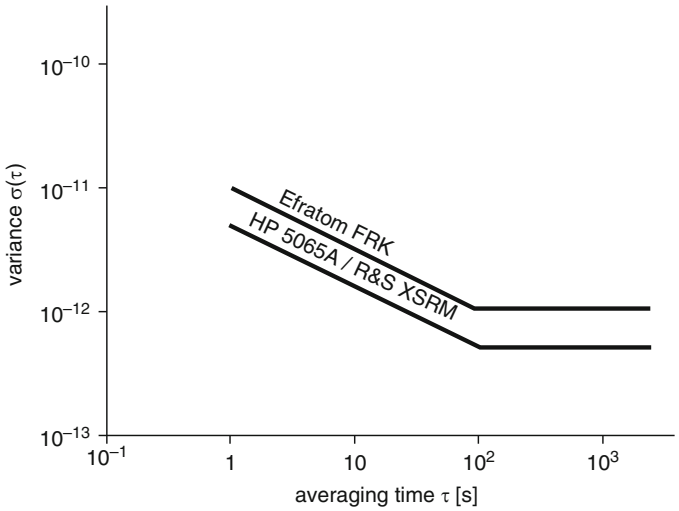

Fig. 2.14 Frequency stability of commercial Rb standards

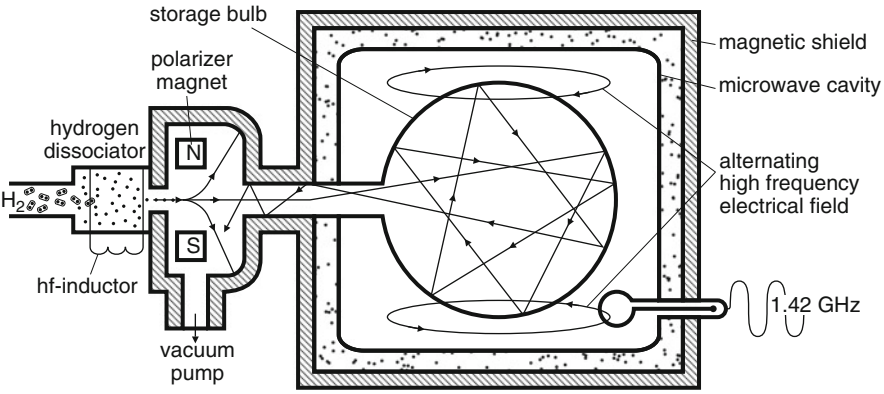

Fig. 2.15 Schematical diagram of a hydrogen maser

coated, e.g., with Teflon to increase the lifetime of atoms in the upper level after being reflected by the wall of the bulb. The vessel is placed inside of a magnetically shielded microwave resonator where a high-frequency noise field containing the clock transition is created to excite induced emission. This process leads to maser activity at the resonance frequency that can be gripped from the resonator to stabilize a quartz clock. Figure 2.16 shows the typical stability behavior of an H maser.

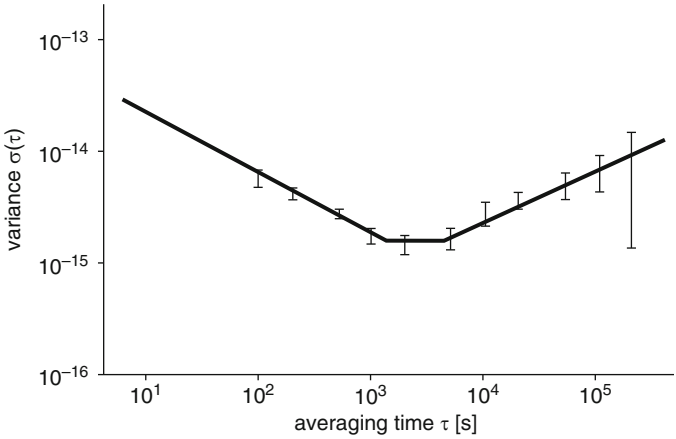

Fig. 2.16 Typical stability behavior of an H maser

2.7 Fountain Clocks

The precision and stability of atomic clocks can be improved by cooling the relevant reference atoms to sub-Kelvin temperatures and thereby reducing their thermal motion significantly. Neutral atoms can be kept by interaction with laser light in optical traps where they can be cooled and further manipulated. In that way it is possible to create fountain clocks where, e.g., Cs atoms are cooled to a few microkelvins and catapulted about a meter upwards in the gravity field of the Earth where in course of their parabolic orbit, they move twice through a microwave resonator. The advantage lies in the long duration time inside the resonator leading to a resonance width of less than 1 Hz. The first cesium fountain clock has been built by LNE-SYRTE at Paris Observatory in 1995 (see, e.g., http://tycho.usno.navy.mil/cesium.html). The clock at Paris Observatory is depicted in Fig. 2.17. Current fountain clocks achieve stabilities of better than 10^{-15}.

2.8 Optical Clocks

Though cesium clocks especially in the form of fountains achieve a remarkable level of stability, their limitations can clearly be seen. A stability of about 10^{-15} can be achieved only after averaging over a day which presents a problem for real-time applications. Now the achievable stability of an atomic clock is related with the clock frequency that for cesium clocks lies in the microwave region at 9.2 GHz. Meanwhile optical clocks have been manufactured with clock frequencies of about 10^{15} Hz, where comparable stabilities can be achieved already after a second. Likely in the near future optical clocks will be superior to conventional atomic clocks. The energy levels of an optical clock are depicted in Fig. 2.18 (left).

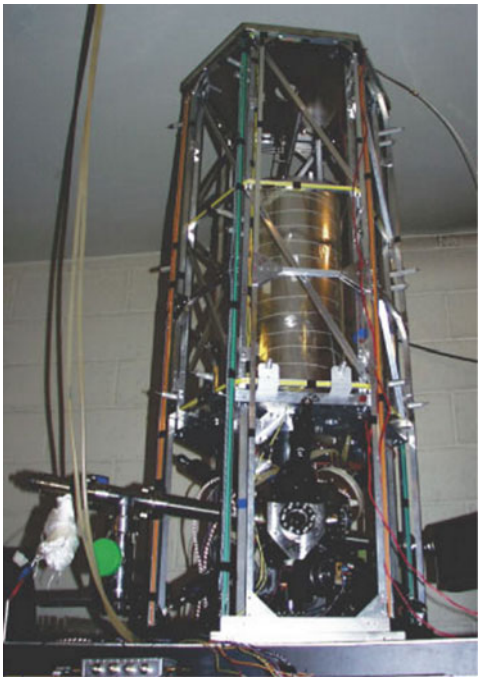

Fig. 2.17 Cs fountain clock at Paris Observatory

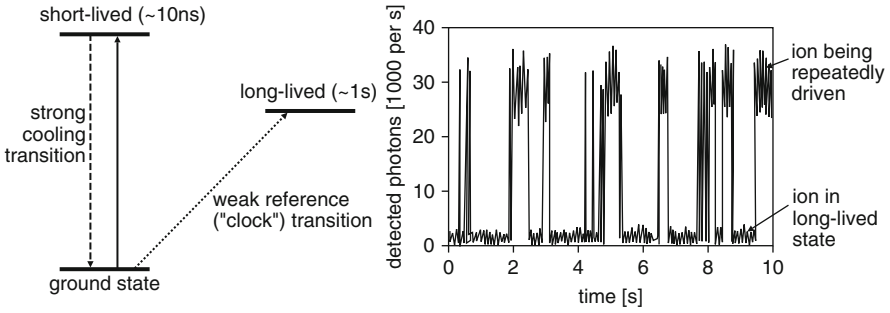

Fig. 2.18 Energy levels of an optical clock (*left*). The cooling transition is accompanied by the emission of fluorescence light (*right*); from http://physicsworld.com (4 May 2005)

An optical clock consists of three main elements: (1) an optical clock transition, (2) a local oscillator, and (3) some counter. In addition we face further elements like traps for atoms or ions, laser for cooling, etc.

1. The first basic element is a precise reference frequency delivered by some very narrow absorption line. Meanwhile a natural line width of less than 1 Hz has

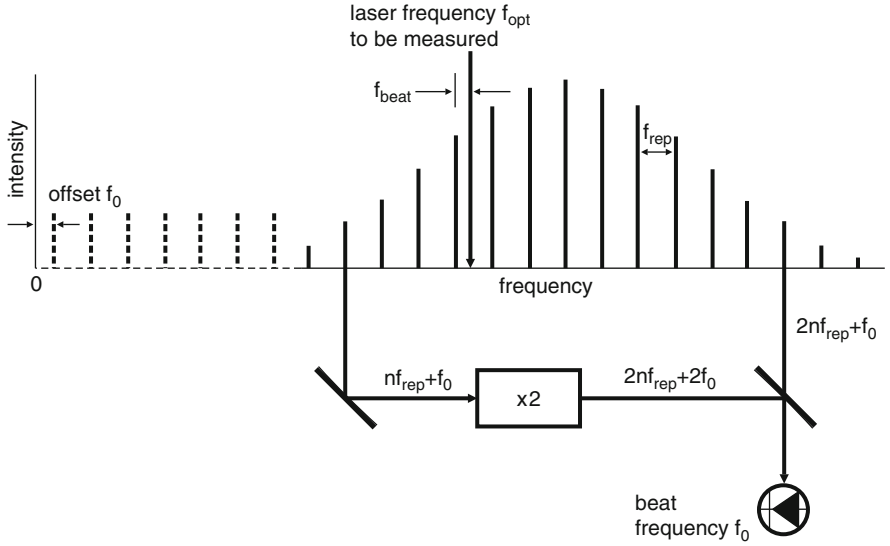

Fig. 2.19 The femtosecond comb in frequency range; from http://physicsworld.com, (4 May 2005)

been achieved for this clock transition, where ions such as $^{199}Hg^+$ or $^{171}Yb^+$ were used.
2. The second main element is a test laser (local oscillator) with a very small bandwidth.
3. Finally, the third basic element is a device that can count the extremely rapid oscillations of the local oscillator.

Critical is the clock transition whose line width should be as narrow as possible. Nowadays, it can be realized by a single ion captured in some electromagnetic trap and laser cooled to less than 1 mK. This clock transition is then probed with monochromatic laser light with a line width of less than 1 Hz. Because of the small line width of the clock transition, the absorption of test photons is very weak; for that reason, a technique called electron shelving comes into play. Laser cooling of the ion is realized by means of some short-living energy level, and during phases of cooling, the electron state oscillates rapidly between this state and the ground state which is accompanied with the emission of fluorescence photons (Fig. 2.18, right). If the test laser, however, hits the clock frequency, the electron enters a long-living state, and the fluorescence light discontinues which is easy to detect.

Since the local oscillator oscillates with a period in the region of a femtosecond, the construction of a counter really presents a challenge. Only in 1999, Ted Hänsch and colleagues succeeded to construct such a counter. It consists of a femtosecond laser that emits a whole train of pulses with a repetition frequency f_{rep} of some

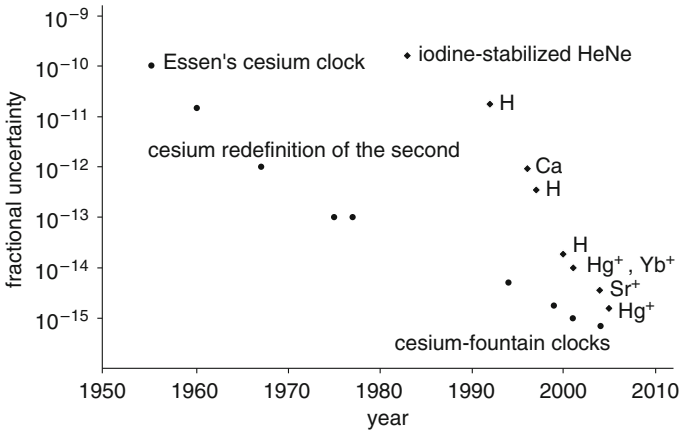

Fig. 2.20 Comparison of achievable stabilities of cesium clocks (*dots*) and optical clocks (*diamonds*)

100 MHz. In that frequency domain, this sequence of pulses appears as a series of equidistant frequencies with separation f_{rep} (Fig. 2.19). For that reason, such a counter is called femtosecond comb. The frequency of a line of such a comb is given by nf_{rep} plus a displacement f_0. Both frequencies f_{rep} and f_0 can be measured by means of beats. Now the comb can be coupled with a cesium clock, and the beat frequency between f_{opt} and the neighboring comb mode can be determined. Meanwhile, it has been shown that optical frequencies can be compared with a femtosecond comb at the level of 10^{-19}. Figure 2.20 shows a comparison of achievable stabilities of cesium and optical clocks.

2.9 Application of Highly Precise Clocks

Figure 2.21 shows the requirements on frequency stability for different modern geodetical methods (EDM: electromagnetic distance measurement; SLR: satellite laser ranging; GPS: global positioning system; LLR: lunar laser ranging; VLBI: very long baseline interferometry). Due to their unrivaled long-term stability (3 h to months), industrial cesiums are used for the generation of national times. Moreover, they are used in mobile SLR systems and the GPS. Rb standards are often used as secondary frequency standards. Because of their good short-term stability, they are also used in SLR, LLR, Doppler, and GPS measurements. Due to their distinguished short-term stability, H masers are employed, e.g., for VLBI measurements.

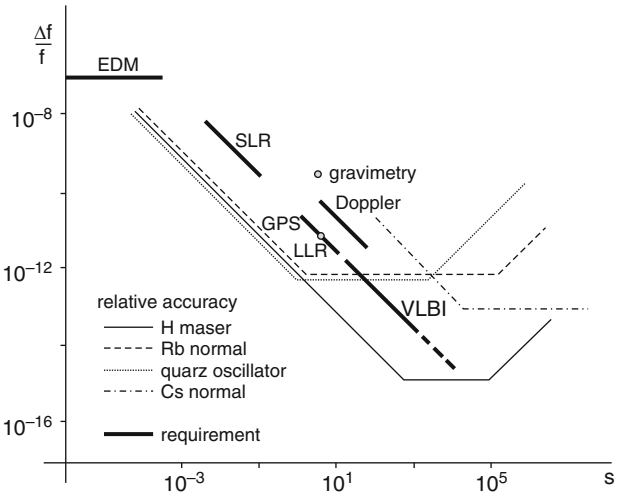

Fig. 2.21 Requirements on frequency stability of several geodetic measuring techniques

2.10 Relativity and the Metric Tensor

Based on the presently achievable stabilities and accuracies of atomic clocks, relativistic effects have to be considered inevitably. The theory of relativity is based upon certain principles that have been verified experimentally with highest precision. The principle of the constancy of the velocity of light in vacuum plays a central role. This principle comprises several independent aspects. First of all the velocity of light in vacuum is independent to the source's state of motion, similar to the sound speed that is also independent upon the velocity of the acoustic source. Then the velocity of light is independent of frequency and polarization. The vacuum is not dispersive. It is common to designate the speed of light in vacuum by c. The numerical value of $c = 299\,792\,458\,\mathrm{m/s}$ is meanwhile used for a definition of the meter.

The meter is the base unit of length in the International System of Units (SI). Originally intended to be one ten-millionth of the distance from the Earth's equator to the North Pole at sea level, its definition has been periodically redefined (Wikipedia). In 1889 at the first General Conference on Weights and Measures (CGPM: Conférence Générale des Poids et Mesures), it was decided to define the SI meter via a prototype (Fig. 2.22) made from a platinum-iridium alloy which was kept at BIPM in Sèvres near Paris. This prototype defined the meter till 1960, when the meter definition was based upon a wavelength of krypton-96 radiation.

After 1983, according to the 17th General Conference on Weights and Measures (1983), the meter is defined as that distance that light travels in vacuum during a time interval of $1/299\,792\,458\,\mathrm{s}$.

Fig. 2.22 The old international prototype of the meter: the famous platinum-iridium stick that defined the meter until 1960. Today the meter is defined by the speed of light in vacuum

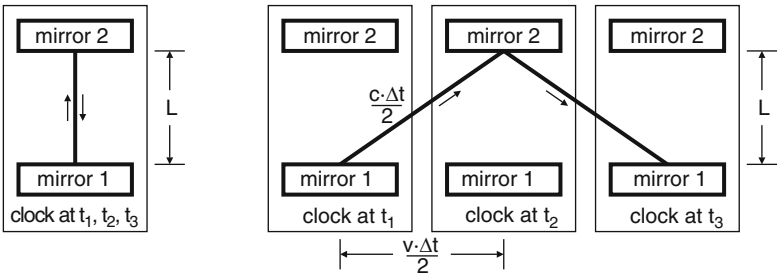

Fig. 2.23 A simple light clock where a light pulse travels between two unaccelerated mirrors back and forth. In the *left part* the observer is at rest with respect to the clock; in the *right part*, the clock moves with velocity v with respect to the observer

Now, the velocity of light in vacuum is also independent to the observer's state of motion (in complete contrast to the sanity and reason); otherwise the present definition of the meter would not make much sense. This aspect of light propagation, which has been experimentally confirmed by many Michelson–Morley-type experiments, has a profound consequence for the problem of clock reading that becomes dependent upon the relative state of motion between clock and observer. To demonstrate this we consider a simple light clock that consists only of two ideal mirrors that move unaccelerated without external forces with constant distance L and a light pulse that moves between the two mirrors back and forth. We first consider an observer at rest with respect to this simple clock (Fig. 2.23, left).

Let us denote the time interval between reflection of a pulse at one mirror and its next return by $\Delta\tau$:

$$\Delta\tau = \frac{2L}{c}.$$

This time interval $\Delta\tau$ is called *proper time interval*. In Fig. 2.23 (right), the same clock is depicted as seen from an observer that moves with the velocity v to the left in the direction of the mirror extensions. It is crucial that also for this observer, light moves with velocity c in vacuum just as for the co-moving observer. Using the Pythagorean theorem, one finds for the corresponding time interval Δt that the moving observer experiences

$$L^2 + \left(\frac{v \cdot \Delta t}{2}\right)^2 = \left(\frac{c \cdot \Delta t}{2}\right)^2,$$

leading to

$$\Delta t = \frac{\Delta\tau}{\sqrt{1 - v^2/c^2}}. \tag{2.16}$$

The observed indication of a clock depends upon the clock's velocity with respect to the observer.

Exercise 2.1: Bill, a 6-year-old boy, is a tennis wizard. Being bored in a railway car, he plays with his tennis ball. He hits the ball hard perpendicular to the floor so that it will be reflected not only by the floor but also from the ceiling in vertical direction and it (almost) comes back to the same point on the ground. His father Ernesto, a physics professor from Stanford University, meditates about the tennis ball: let L be the height of the wagon, then the time it takes for the tennis ball to move from the bottom to the ceiling and back is $\Delta\tau = 2L/v_\mathrm{T}$, if v_T is the velocity of the tennis ball. Suppose the train moves with constant speed v with respect to the train station in Hayward. Show that some observer standing on the platform of the train station measures the same time interval as professor Ernesto, i.e., $\Delta t = \Delta\tau$.

The metric tensor has turned out to be a very efficient tool for the description of light propagation and clock rates. For its introduction we first describe a certain part of space, together with time, by means of 4-dimensional space–time coordinates $x^\mu = (ct, x^i)$. The variable t designates the time coordinate that is related with the space–time coordinate $x^0 = ct$.

We want to declare that a Greek index like μ indicates a space–time index that runs over the values $0, 1, 2, 3$. The index 0 refers to the time coordinate ($x^0 = ct$); the indices $1, 2, 3$ describe the three spatial coordinates (e.g., $x^1 = x, x^2 = y$ and $x^3 = z$). Such coordinates label certain events in space–time. An event is some instance that has only a small extension in space and time. Now we consider two infinitesimally close events e_1 and e_2 with coordinates $e_1 : x^\mu$ and $e_2 : x^\mu + \mathrm{d}x^\mu$. The space–time distance $\mathrm{d}s$ between these two neighboring events is then given by

$$\mathrm{d}s^2 = g_{\mu\nu}\,\mathrm{d}x^\mu \mathrm{d}x^\nu, \tag{2.17}$$

where $g_{\mu\nu}$ is the metric tensor. In (2.17), we have used the usual Einstein summation convention saying that over two identical (dummy) indices, a summation is implied automatically; in this case, a summation over μ and $\nu, \mu, \nu = 0, 1, 2, 3$ is assumed automatically. The metric tensor $g_{\mu\nu}$ can be viewed as a 4×4 matrix with components $g_{00}, g_{01}, \ldots, g_{10}, g_{11}, \ldots$, etc. In the 3-dimensional Euclidean space with Cartesian coordinates $x^i = x, y, z$, the metric tensor is simply given by $g_{ij} = \mathrm{diag}(1, 1, 1)$, i.e., the length element takes the form

$$\mathrm{d}s^2 = \mathrm{d}x^2 + \mathrm{d}y^2 + \mathrm{d}z^2,$$

which is nothing but the infinitesimal version of the Pythagorean theorem.

Without gravitational fields we can introduce inertial Cartesian coordinates $x^\mu = (ct, \mathbf{x})$ such that the metric tensor takes the form

$$g_{\mu\nu} = \mathrm{diag}(-1, 1, 1, 1) \tag{2.18}$$

and the corresponding length element reads

$$\mathrm{d}s^2 = -c^2\mathrm{d}t^2 + \mathrm{d}\mathbf{x}^2. \tag{2.19}$$

We would like to stress that the length element is negative in the direction of time and positive for spatial separations. In this way there is always a clear distinction between time and space. With the line element we can describe the propagation of light rays and clock rates in a very simple manner. Light rays are simply curves with

$$\mathrm{d}s^2 = 0\,. \qquad \text{(light propagation)} \tag{2.20}$$

This ensures the complete principle of the constancy of the velocity of light in vacuum as discussed above. We now consider a clock with coordinates $\mathbf{x}_\mathrm{c}(\tau)$ where τ is the proper time, i.e., the time an observer co-moving with the clock reads. The curve $(c\tau, \mathbf{x}_\mathrm{c}(\tau))$ is called the world line of our (idealized) clock. Let $\mathrm{d}s$ be an infinitesimal element of this world line; then the proper time of the clock, $\mathrm{d}\tau$, can be obtained by

$$\mathrm{d}\tau^2 = -\frac{1}{c^2}\mathrm{d}s^2 = -\frac{1}{c^2}g_{\mu\nu}\mathrm{d}x_c^\mu \mathrm{d}x_\mathrm{c}^\nu. \tag{2.21}$$

For a clock moving with velocity $\mathbf{v}$, we get from (2.19)

$$\mathrm{d}\tau^2 = \mathrm{d}t_\mathrm{c}^2 - \frac{1}{c^2}\mathrm{d}\mathbf{x}_\mathrm{c}^2 = \mathrm{d}t_\mathrm{c}^2\left(1 - \frac{\mathbf{v}^2}{c^2}\right) \tag{2.22}$$

in accordance with relation (2.16).

Exercise 2.2: The coordinate time interval of a clock Δt_c is 1 s, and its velocity is 30 km/s. What is the difference between the proper time and coordinate time interval?

Exercise 2.3: Let us consider the 2-dimensional Euclidean plane with Cartesian coordinates (x, y) and basis vectors $\mathbf{e}_x$ and $\mathbf{e}_y$. Define $\mathbf{e}_{x'} = \mathbf{e}_x$ and $\mathbf{e}_{y'}$, a unit vector inclined by an angle α with respect to $\mathbf{e}_x$. Construct coordinates (x', y') such that

$$\mathbf{v} = x\mathbf{e}_x + y\mathbf{e}_y = x'\mathbf{e}_{x'} + y'\mathbf{e}_{y'}.$$

Compute the components of the metric tensor in the primed coordinates from $\mathrm{d}s^2 = \mathrm{d}x^2 + \mathrm{d}y^2$.

2.11 Lorentz Transformation

We now consider some inertial system with coordinates $(ct, \mathbf{x})$ and a second one with coordinates $(cT, \mathbf{X})$ whose origin moves with velocity $\mathbf{v}$ with respect to the first system. According to the above, the line element in the first system is given by

$$\mathrm{d}s^2 = -c^2\mathrm{d}t^2 + \mathrm{d}\mathbf{x}^2$$

and in the second (moving) inertial system by

$$\mathrm{d}s^2 = -c^2\mathrm{d}T^2 + \mathrm{d}\mathbf{X}^2.$$

Now, $\mathrm{d}s^2$ is a coordinate-independent geometrical length element, so the right hand sides of the last two equations have to agree. This form invariance of the metric tensor (i.e., identical components of the metric tensor) if we go from one inertial system to another leads to the form of the coordinate transformation from $x^\mu = (ct, \mathbf{x})$ to $X^\alpha = (cT, \mathbf{X})$:

$$X^\alpha = \Lambda^\alpha_\beta \, x^\beta \tag{2.23}$$

with

$$\begin{aligned} \Lambda^0_0 &= \gamma \\ \Lambda^0_i &= \Lambda^i_0 = -\gamma\beta^i \\ \Lambda^i_j &= \delta_{ij} + \frac{v^i v^j}{v^2}(\gamma - 1) \end{aligned} \tag{2.24}$$

and

$$\gamma \equiv (1 - \beta^2)^{-1/2}, \qquad \beta^i = v^i/c. \tag{2.25}$$

The transformation (2.23) and (2.24) is called *Lorentz transformation*. Explicitly we have

$$cT = \Lambda^0_\beta x^\beta = \Lambda^0_0 ct + \Lambda^0_i x^i$$

or

$$T = \gamma \left(t - \frac{\mathbf{v} \cdot \mathbf{x}}{c^2} \right) . \tag{2.26}$$

The spatial coordinates transform according to

$$X^i = \Lambda^i_\beta x^\beta = \Lambda^i_0 ct + \Lambda^i_j x^j$$

or

$$\mathbf{X} = \mathbf{x} - \gamma \mathbf{v} t + (\gamma - 1) \frac{\mathbf{v}(\mathbf{v} \cdot \mathbf{x})}{v^2}. \tag{2.27}$$

For the special case that the velocity $\mathbf{v}$ points into x-direction, we have

$$\begin{aligned} T &= \gamma \left(t - \frac{vx}{c^2} \right) \\ X &= \gamma (x - vt) \end{aligned} \tag{2.28}$$

or

$$\begin{aligned} t &= \gamma \left(T + \frac{vX}{c^2} \right) \\ x &= \gamma (X + vT) \end{aligned} \tag{2.29}$$

and $Y = y, Z = z$. The following exercise shows that the Lorentz transformation leads indeed to the invariance of the line element.

Exercise 2.4: In some inertial system (the rest system) with coordinates $x^\mu \equiv (ct, \mathbf{x})$, the metric tensor is given by $\mathrm{d}s^2 = -c^2 \mathrm{d}t^2 + \mathrm{d}\mathbf{x}^2$. A second inertial system with coordinates $X^\alpha \equiv (cT, \mathbf{X})$ and the metric tensor $\mathrm{d}S^2 = -c^2 \mathrm{d}T^2 + \mathrm{d}\mathbf{X}^2$ moves with constant velocity along the common x-axes with velocity v. Let the moving coordinates be related with those of the rest system by a Lorentz transformation (2.28). Show that under these conditions $\mathrm{d}S^2 = \mathrm{d}s^2$.

Of interest is an expansion of the Lorentz transformation in powers of $1/c$. With

$$\gamma = 1 + \frac{1}{2}\beta^2 + \frac{3}{8}\beta^4 + \mathcal{O}(\beta^6)$$

we obtain

$$\begin{aligned} T &= t \left(1 + \frac{1}{2}\beta^2 + \frac{3}{8}\beta^4 \right) - \left(1 + \frac{1}{2}\beta^2 \right) \frac{\mathbf{v} \cdot \mathbf{x}}{c^2} + \mathcal{O}(c^{-5}), \\ \mathbf{X} &= \mathbf{x} - \left(1 + \frac{1}{2}\beta^2 \right) \mathbf{v} t + \frac{1}{2} \frac{\mathbf{v}(\mathbf{v} \cdot \mathbf{x})}{c^2} + \mathcal{O}(c^{-4}). \end{aligned} \tag{2.30}$$

2.12 Geocentric Timescales TCG, TT, TAI, and UTC

The frequency standards described above generate ultrastable oscillations that are counted; converted into hours, minutes, and seconds; and are finally displayed. The quality of a clock depends essentially upon two quantities: (1) its stability and (2) its accuracy. The stability usually described by means of the two-point Allan variance gives a measure of frequency fluctuations as function of averaging time. On the other hand, accuracy describes the ability to realize the SI second.

The SI second is defined as the duration of 9 192 631 779 periods of the radiation that the ^{133}Cs atom at rest emits during the corresponding hyperfine transition.

An individual clock primarily delivers a free timescale. The readings of several clocks can be related with a suitable synchronization procedure. In practice the geocentric coordinate time is used to synchronize clocks in the vicinity of the Earth. Let (T, X^a) be geocentric nonrotating quasi-inertial coordinates (the acceleration of the geocenter will not play an important role for the following). The geocentric coordinate time T is also called

$$T = \mathrm{TCG}.$$

Actual clocks in the vicinity of the Earth do not show the time $T = \mathrm{TCG}$ but their proper time that is related with TCG by

$$c^2 \mathrm{d}\tau^2 = \left(1 - \frac{2U}{c^2}\right) c^2 \mathrm{d}T^2 - \mathrm{d}\mathbf{X}^2.$$

In this equation U denotes the Newtonian gravitational potential. By means of relation (2.21), we might interpret this relation by writing the metric tensor in geocentric quasi-inertial Cartesian coordinates in the form

$$\mathrm{d}s^2 = -\left(1 - \frac{2U}{c^2}\right) c^2 \mathrm{d}T^2 + \mathrm{d}\mathbf{X}^2. \tag{2.31}$$

Neglecting higher-order terms in $(1/c)$, we can solve this equation for $\mathrm{d}\tau/\mathrm{d}T$:

$$\begin{aligned} c^2 \mathrm{d}\tau^2 &= c^2 \mathrm{d}T^2 \left[1 - \frac{2U}{c^2} - \frac{1}{c^2}\left(\frac{\mathrm{d}\mathbf{X}}{\mathrm{d}T}\right)^2\right] \\ &= c^2 \mathrm{d}T^2 \left[1 - \frac{2U}{c^2} - \frac{\mathbf{V}^2}{c^2}\right] \end{aligned}$$

or

$$\frac{\mathrm{d}\tau}{\mathrm{d}T} = \left[1 - \frac{2U}{c^2} - \frac{\mathbf{V}^2}{c^2}\right]^{1/2}. \tag{2.32}$$

Here, $\mathbf{V}$ is the geocentric coordinate (GCRS) velocity of the clock. A Taylor expansion $(1-x)^{1/2} = 1 - x/2 + \cdots$ finally yields

$$\frac{\mathrm{d}\tau}{\mathrm{d}T} \simeq 1 - \frac{U}{c^2} - \frac{1}{2}\frac{\mathbf{V}^2}{c^2}. \tag{2.33}$$

The U-term in this relation results from the *gravitational redshift* (the wavelength of a photon increases if it moves upwards in a gravitational field) implying that an atomic clock is slowed down in a gravitational field. The $\mathbf{V}^2$-term results from the quadratic Doppler effect implying that a fast-moving clock apparently is slowed down. This last effect, however, is relative; for an observer that is co-moving with the clock, a clock at rest would appear to be slowed down.

We will now switch from our quasi-inertial coordinates to coordinates $\overline{\mathbf{X}}$ that are co-rotating with the Earth. With

$$\mathbf{V} = \boldsymbol{\Omega} \times \overline{\mathbf{X}} + \overline{\mathbf{V}},$$

where $\overline{\mathbf{V}}$ is the clock's velocity in the rotating system, we have

$$c^2\mathrm{d}\tau^2 = c^2\mathrm{d}T^2 \left[1 - \frac{2U_{\mathrm{geo}}}{c^2} - 2(\boldsymbol{\Omega} \times \overline{\mathbf{X}}) \cdot \frac{\overline{\mathbf{V}}}{c^2} - \frac{\overline{\mathbf{V}}^2}{c^2}\right], \tag{2.34}$$

where

$$U_{\mathrm{geo}} = U + \frac{1}{2}(\boldsymbol{\Omega} \times \overline{\mathbf{X}})^2$$

is the geopotential that consists of the gravitational potential of the Earth and the centrifugal potential. $\boldsymbol{\Omega}$ is the angular velocity of the Earth. For earthbound clocks with $\mathrm{d}\overline{\mathbf{X}} = 0 = \overline{\mathbf{V}}$, we get

$$\frac{\mathrm{d}\tau}{\mathrm{d}T} = 1 - \frac{U_{\mathrm{geo}}}{c^2} = 1 - \frac{U_0}{c^2} + \frac{g(\psi)\cdot h}{c^2} + \cdots. \tag{2.35}$$

Here $U_0 = U_{\mathrm{geo}}(\mathrm{geoid}) = \mathrm{const.}$ denotes the geopotential on the geoid, ψ is geographic latitude, and $g(\psi)$ is the gravity acceleration on the geoid:

$$g(\psi) = (9.78027 + 0.05192\sin^2\psi) \times 10^2\,\mathrm{cm/s^2} \quad \text{and}$$

h denotes the clock's height above the geoid. For two earthbound clocks, we have

$$\begin{aligned}\frac{(\mathrm{d}\tau)_1}{(\mathrm{d}\tau)_2} = \frac{f_2}{f_1} &= \frac{(1 - U_{\mathrm{geo}}/c^2)_1}{(1 - U_{\mathrm{geo}}/c^2)_2} = \frac{(1 - U_0/c^2 + g(\psi)\cdot h/c^2)_1}{(1 - U_0/c^2 + g(\psi)\cdot h/c^2)_2} \\ &\simeq \frac{(1 + g(\psi)\cdot h/c^2)_1}{(1 + g(\psi)\cdot h/c^2)_2}.\end{aligned}$$

As an example we consider a first clock at the PTB (Physikalisch Technische Bundesanstalt) in Brunswick, Germany, with $h = 73\,\mathrm{m}$ and $gh/c^2 = 8 \cdot 10^{-15}$ and a second one at NIST (US National Institute of Standards and Technology, Boulder, Colorado, USA) with $h = 1,634\,\mathrm{m}$ and $gh/c^2 = 2 \cdot 10^{-13}$. The difference in clock rates is given by

$$f_{\mathrm{PTB}} \simeq (1 + 2 \cdot 10^{-13})\, f_{\mathrm{NBS}}.$$

This leads to a difference of $5.4\,\mu\mathrm{s}$ that has accumulated during the time span of 1 year.

Exercise 2.5: If somebody put an atomic clock on top of Mount Everest (geographic latitude: $27°\,59'\,17''$N, height: $8,844\,\mathrm{m}$) and compares the clock readings with that of an atomic clock of PTB in Brunswick (geographic latitude: $52°\,17'\,40''$N, height: $73\,\mathrm{m}$), what would be the time offset after 1 year?

The definition of the SI second makes it clear that it is defined first of all for proper times. However, if we have a well-defined relation between some coordinate time and proper time, the SI second will be the induced time unit also for some coordinate time. This especially applies for terrestrial time (TT) and international atomic time (TAI).

Let TT be a timescale differing from $T = \mathrm{TCG}$ only by a constant rate. This rate should agree at some level of approximation with that of a clock located on the geoid. For earthbound clocks, we had

$$\frac{\mathrm{d}\tau}{\mathrm{d}T} \simeq 1 - \frac{U_0}{c^2} + \frac{g(\psi) \cdot h}{c^2}.$$

On the geoid with $h = 0$, we have

$$\mathrm{d}\tau = \left(1 - \frac{U_0}{c^2}\right) \mathrm{d}T = k_E\, \mathrm{d}T \equiv \mathrm{d(TT)}$$

with

$$k_E = 1 - \frac{U_0}{c^2}.$$

Thus we have the relation

$$\mathrm{TT} = k_E\, T = k_E\, \mathrm{TCG}. \tag{2.36}$$

For presently achievable clock accuracies the precise definition and realization of the geoid, however, presents a problem. For that reason, the timescales TT and TAI are related with TCG by a defining constant k_E:

$$k_E = 1 - 6.969290134 \times 10^{-10}.$$

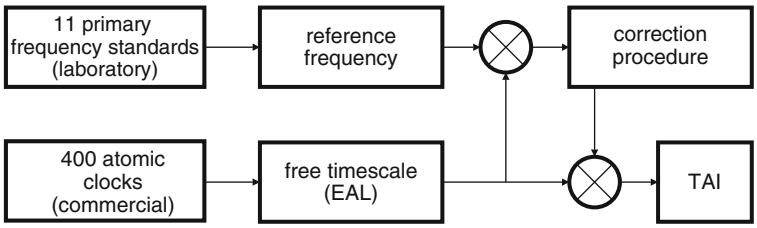

Fig. 2.24 Scheme how TAI is realized

Due to their stochastic properties actual clocks do not exactly show idealized proper time τ. International atomic time (Temps Atomique International) is therefore derived from a mean value over the readings of many individual atomic clocks. We write

$$\frac{\mathrm{d}\tau}{\mathrm{d}T} \simeq 1 - \frac{1}{c^2}\,(U_0 + U_R)$$

with

$$U_R = -g(\psi) \cdot h + \cdots .$$

Then TAI is defined as the mean value

$$\mathrm{TAI} = \frac{1}{N}\sum_{i=1}^{N}(\tau_i + S_i/c^2)$$

with

$$S_i = \int_{T_0}^{T} U_R \,\mathrm{d}T'.$$

Here, the index i labels the various atomic clocks used for the realization of TAI. The second term in the TAI definition simply indicates that the readings of some clock have to be transferred to the geoid before the averaging over the various clocks is taken.

Presently the readings of about 400 clocks in 68 laboratories are employed for the realization of TAI (Fig. 2.24). These clocks are:

- Standard Cs clocks with stabilities of 5×10^{-14} for an averaging time of about 5 days and accuracies of about 10^{-12},
- Highly precise Cs standards with stabilities of 1×10^{-14} for an averaging time of about 5 days and accuracies of 5×10^{-13}, as well as
- H maser with stabilities of about 7×10^{-16} for an averaging time of about 1 day.

These atomic clocks first define a free timescale called Echelle Atomique Libre (EAL). From the EAL, the frequency of TAI is finally tuned by a few number of primary frequency standards (PFS). The TAI zero point was fixed to TAI = UT1

for 1 January 1958, 0^h. Presently the PFS are located at LNE-SYRTE, Laboratoire National de Métrologie et d'Essais, Paris, France; INRIM, Istituto Nazionale di Ricerca Metrologia, Torino, Italy; NIST, National Institute of Standards and Technology, Boulder (Colorado), USA; NPL, National Physical Laboratory, Middlesex, GB; and PTB, Physikalisch Technische Bundesanstalt, Brunswick, Germany:

- LNE-SYRTE-F01 (Cs fountain)
- LNE-SYRTE-FO2 (Cs/Rb fountain)
- LNE-SYRTE-FOM (transportable Cs fountain)
- LNE-SYRTE-JPO (optically pumped Cs beam)
- IT-CSF1, INRIM (Cs fountain)
- NIST-F1 (Cs fountain)
- NPL-CSF2 (Cs fountain)
- PTB-CS1 (Cs beam, continuous operation)
- PTB-CS2 (Cs beam, continuous operation)
- PTB-CSF1 (Cs fountain)
- PTB-CSF2 (Cs fountain)

A single clock produces a free timescale. A relation between two such timescales can be established easily if the two clocks are placed in immediate vicinity so that the two clocks can be read off simultaneously. The notion of *simultaneity*, however, rests on a convention for spatially separated clocks. Einstein has discussed a special synchronization procedure for well-separated clocks by means of electromagnetic signals; e.g., by means of an observer that is placed in the middle between the two clocks and simultaneously emits two light signals towards the two clocks that by definition arrive there simultaneously. However, it can be shown that (due to the Sagnac effect in time that is discussed below) a clock synchronization according to Einstein is not possible on the rotating Earth. This point will now be discussed more extensively.

One defines that two clocks showing proper times τ_1 and τ_2 are called synchronous if the corresponding $T = \mathrm{TCG}$ agree, i.e., if $T_1 = T_2$. Since this kind of clock synchronization employs the coordinate time $T = \mathrm{TCG}$, it is also called coordinate time synchronization. According to the above we have

$$\mathrm{d}\tau \simeq \mathrm{d}T \left[1 - \frac{U_{\mathrm{geo}}}{c^2} - \frac{1}{2}\frac{\overline{\mathbf{V}}^2}{c^2} - \frac{(\boldsymbol{\Omega} \times \overline{\mathbf{X}}) \cdot \overline{\mathbf{V}}}{c^2} \right]$$

or with $(1 + x)^{-1} = 1 - x + \cdots$

$$\Delta T \simeq \int \mathrm{d}\tau \left[1 + \frac{U_{\mathrm{geo}}}{c^2} + \frac{1}{2}\frac{\overline{\mathbf{V}}^2}{c^2} + \frac{(\boldsymbol{\Omega} \times \overline{\mathbf{X}}) \cdot \mathbf{V}}{c^2} \right]. \tag{2.37}$$

The synchronization of earthbound clocks can be achieved by means of a clock transport. For a slow transport ($\overline{\mathbf{V}}^2 \sim 0$) at low altitudes ($h \sim 0$), we have

$$\begin{aligned}\Delta(\mathrm{TT}) &\simeq \left(1-\frac{U_0}{c^2}\right)\Delta T \simeq \int \mathrm{d}\tau \left[1+(\boldsymbol{\Omega}\times\overline{\mathbf{X}})\frac{\overline{\mathbf{V}}}{c^2}\right] \\ &\simeq \Delta\tau + \frac{\Omega R_\mathrm{E}}{c^2}\int \mathrm{d}\tau\, v_\mathrm{east}\cos\psi,\end{aligned} \tag{2.38}$$

where v_east is the eastward component of $\overline{\mathbf{V}}$. For a transport along a meridian with $v_\mathrm{east} = 0$, we simply get $\Delta(TT) = \Delta\tau$. For a transport along a parallel, we get

$$\Delta(\mathrm{TT}) \simeq \Delta\tau + \frac{\Omega R_\mathrm{E}}{c^2} L_\mathrm{east}\cos\psi,$$

if L_east denotes the distance covered in eastward direction. We now consider two events of clock comparison: one before and one after the transport of a clock. For both events the TCG or TT value will be the same for the two clocks. However, for the stationary clock $\Delta\tau = \Delta(\mathrm{TT})$, whereas the elapsed proper time of the transported clock will be shorter by 207 ns by the Sagnac effect in time if it was moved once around the Earth along the equator in eastward direction.

For practical reasons also, TT is derived from atomic time TAI. The IAU has decided that

$$\mathrm{TT} = \mathrm{TAI} + 32.184\,\mathrm{s}.$$

The constant 32.184 s is simply a convention that was chosen for historical reasons.

We now come to the important definition of coordinated universal time UTC. It is primarily an atomic time. Later we will introduce so-called Earth's timescales that strictly speaking are not physical timescales but angles related with the Earth's orientation in space. UT1 is such a timescale that will be introduced later. Now, UTC is defined to differ from TAI by a certain integral number of (leap) seconds, i.e.,

$$\mathrm{TAI} = \mathrm{UTC} + N\,\mathrm{s}\,,$$

if N denotes a positive integer. Since 1 January 1972 is defined by the introduction of leap seconds so that the difference $|\mathrm{UTC} - \mathrm{UT1}|$ is always smaller than 0.9 s,

$$|\mathrm{UTC} - \mathrm{UT1}| < 0.9\,\mathrm{s}.$$

This has the advantage that over a very long time span, UTC that is related with the Sun via the Earth's orientation in space will remain useful for ordinary life. Since 1972, a leap second is introduced with preference at 30 June or 31 December of a year, always at $23^\mathrm{h}59^\mathrm{m}59^\mathrm{s}$ UTC. This way a new offset between UTC and UT1 is valid at $0^\mathrm{h}00^\mathrm{m}00^\mathrm{s}$ of 1 July or 1 January respectively. Table 2.1 shows the instants of time when new leap second values became valid. The *AstroRef* function `GetLeapSeconds` returns the number of leap seconds valid for a given JD_UTC. The offset between UT1 and UTC is denoted

$$\Delta\mathrm{UT1} = \mathrm{UT1} - \mathrm{UTC}$$

Table 2.1 Moments of time where new offsets N (TAI-UTC in seconds) between TAI and UTC became valid by the introduction of leap seconds

Julian date	Date	N	Julian date	Date	N
JD 2441317.5	1 Jan 1972	+10	JD 2446247.5	1 Jul 1985	+23
JD 2441499.5	1 Jul 1972	+11	JD 2447161.5	1 Jan 1988	+24
JD 2441683.5	1 Jan 1973	+12	JD 2447892.5	1 Jan 1990	+25
JD 2442048.5	1 Jan 1974	+13	JD 2448257.5	1 Jan 1991	+26
JD 2442413.5	1 Jan 1975	+14	JD 2448804.5	1 Jul 1992	+27
JD 2442778.5	1 Jan 1976	+15	JD 2449169.5	1 Jul 1993	+28
JD 2443144.5	1 Jan 1977	+16	JD 2449534.5	1 Jul 1994	+29
JD 2443509.5	1 Jan 1978	+17	JD 2450083.5	1 Jan 1996	+30
JD 2443874.5	1 Jan 1979	+18	JD 2450630.5	1 Jul 1997	+31
JD 2444239.5	1 Jan 1980	+19	JD 2451179.5	1 Jan 1999	+32
JD 2444786.5	1 Jul 1981	+20	JD 2453736.5	1 Jan 2006	+33
JD 2445151.5	1 Jul 1982	+21	JD 2454832.5	1 Jan 2009	+34
JD 2445516.5	1 Jul 1983	+22	JD 2456109.5	1 Jul 2012	+35

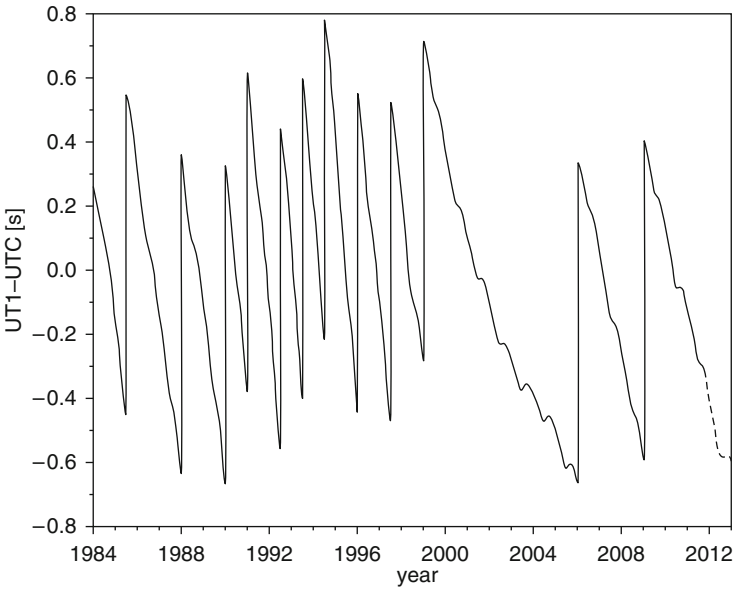

Fig. 2.25 UT1–UTC with extrapolated values (based on data from USNO)

and is continuously determined by the International Earth Rotation and Reference Systems Service (IERS). The *AstroRef* function `GetDeltaUT1` implements access to this data. Using the function `ConvertTime`, it is possible to convert one timescale into another (see appendix B). Finally, Fig. 2.25 shows the difference UT1–UTC for the years 1984 to mid-2012 (extrapolated).

Presently these leap seconds have to be considered for highly precise applications. However, from a practical point of view the introduction of a leap second is related with a considerable expenditure, not only for financial reasons. For that

Fig. 2.26 The division of the Earth into time zones

reason the discussions about leap seconds will continue, and it can very well be that in the future, one might introduce leap hours at larger intervals of time for the difference TAI–UTC.

2.13 Time Zones

The national timescales as well as daylight saving times are based upon UTC. Central European time CET, e.g., is given by

$$\mathrm{CET} = \mathrm{UTC} + 1^{\mathrm{h}} \tag{2.39}$$

and the corresponding daylight saving time (central European summer time) by

$$\mathrm{CEST} = \mathrm{UTC} + 2^{\mathrm{h}}\,. \tag{2.40}$$

Different national times usually differ from UTC by an integer number of hours according to a division into time zones that are depicted in Fig. 2.26.

2.14 Julian Date

In astronomy it has become a usual practice to characterize a certain moment of time by the Julian date (JD). The definition is general enough so that it can be applied to any continuous timescale such as TCG or TT; at highest precision one

has to distinguish JD_{TT} from JD_{TCG} etc. The Julian calendar was introduced by the Romans around the year 46 BC. It is based upon a year of 365 days, but every 4th year that can be divided by the number 4 has an additional leap day. A Julian century therefore has exactly 36, 525 days. In the year 1582 Pope Gregory XIII suggested a new calendar with a mean annual length of 365.2425 days that has only 97 leap years in 400 years (to better approximate the length of the tropical year, the time span between two subsequent equinoxes). In the Gregorian calendar, those years that can be divided by 100 are no leap years with the exception of those that can be divided by 400. Therefore, the years 1800 and 1900 were no leap years, the year 2000 however was. In course of time, all countries that had used the Julian calendar have switched to the Gregorian calendar.

The Julian date is a continuous counting of days and fractions thereof starting from the year $-4712, 12^{\mathrm{h}}$ TT. Let Y be the year, M the month number (1 for January), and D the day possibly either in the Julian or in the Gregorian calendar (notice that 4 October 1582 in the Julian calendar is followed by 15 October 1582 in the Gregorian calendar). The exact moment of time is accounted for by adding fractions of a day in the D value (as digits after the decimal point). The JD algorithm then reads:

1. For $M > 2$, Y and M are left unchanged. For $M = 1$ or 2, Y is replaced by $Y - 1$ and M by $M + 12$.
2. In the Gregorian calendar, one computes

$$A = \mathrm{INT}(Y/100); \qquad B = 2 - A + \mathrm{INT}(A/4)\,,$$

   where INT denotes the integer part of the number (e.g., $\mathrm{INT}(3.92) = 3$). In the Julian calendar, $B = 0$.
3. JD is then given by

$$\mathrm{JD} = \mathrm{INT}(365.25 \cdot (Y + 4716)) + \mathrm{INT}(30.6001 \cdot (M + 1)) + D + B - 1524.5.$$

Of great importance is the date J2000.0 for which

$$\mathrm{J2000.0} = 1\ \text{January}\ 2000,\ 12^{\mathrm{h}} = \mathrm{JD}\,2\,451\,545.0.$$

In the literature one often finds also values for the *modified Julian date* (MJD) that is defined as

$$\mathrm{MJD} = \mathrm{JD} - 2\,400\,000.5.$$

The value $\mathrm{MJD} = 0$ corresponds to 17 November 1858, 0^{h}.

The Maple™function `JDDate` of the supplied *AstroRef* package computes the Julian date from a date in the Julian or Gregorian calendar. The function `CalendarDate` does the inverse transformation (see Appendix B).

Exercise 2.6: Calculate the Julian date JD and modified Julian date MJD for the following instants of time: 30 July 1853, 21 April 1937, 1 February 1977, 1 January 2000, 20 May 2006, 1 June 2011, and for 12^h TT.

Exercise 2.7: Calculate the day of the week when Edmund Halley observed a solar eclipse on 3 May 1715!

Exercise 2.8: Use the function `CalendarDate` to compute the calendar date and time for the following JD values: 2451545.00, 2450313.25, and 2450026.75.

Exercise 2.9: Calculate the Julian date for the ancient solar eclipse 28 May 585 BC!

2.15 Barycentric Timescales TCB, T_{eph}, and TDB

The timescales introduced in the last section are all related with the geocenter; they are geocentric timescales to be used in the vicinity of the Earth. For certain applications, however, such as solar system ephemerides or interplanetary spacecraft navigation, barycentric timescales have to be used where the barycenter refers to the solar system's center of mass. The basic barycentric timescale is barycentric coordinate time TCB. For the definition of TCB, one might image some fictitious clock at the geocenter neglecting the gravity field of the Earth. For this case, the first post-Newtonian relation between TCB and TCG reads

$$\frac{\mathrm{d(TCG)}}{\mathrm{d(TCB)}} \simeq 1 - \frac{U_{\mathrm{ext}}(\mathbf{z}_\mathrm{E})}{c^2} - \frac{1}{2}\frac{\mathbf{v}_\mathrm{E}^2}{c^2}$$

or

$$\Delta(\mathrm{TCG}) \simeq \Delta(\mathrm{TCB}) - \frac{1}{c^2}\left[\int\left(U_{\mathrm{ext}}(\mathbf{z}_\mathrm{E}) + \frac{1}{2}\mathbf{v}_\mathrm{E}^2\right)\mathrm{d}t\right].$$

Here, $t = \mathrm{TCB}$, U_{ext} is the gravitational potential of Sun and planets excluding the Earth and $\mathbf{z}_\mathrm{E}, \mathbf{v}_\mathrm{E}$ the barycentric coordinate position and velocity of the geocenter. For some point $\mathbf{x}$ close to the geocenter, this relation is given by

$$\mathrm{TCB} - \mathrm{TCG} = c^{-2}\left[\int_{t_0}^{t}\left(U_{\mathrm{ext}}(\mathbf{z}_\mathrm{E}) + \frac{1}{2}\mathbf{v}_\mathrm{E}^2\right)\mathrm{d}t' + \mathbf{v}_\mathrm{E}\cdot(\mathbf{x} - \mathbf{z}_\mathrm{E})\right]. \qquad (2.41)$$

The second term on the right hand side results from the fact that two events that are simultaneous with respect to TCB generally are not simultaneous in a geocentric system (i.e., with respect to TCG). The moment of time t_0 where TCB = TCG is given by

$$t_0 = \mathrm{JD}\,2\,443\,144.5\,.$$

TCB and TCG differ not only by periodic terms but also by a secular drift given by

$$(\mathrm{TCB} - \mathrm{TCG})_{\mathrm{sec}} = L_\mathrm{C}(\mathrm{JD} - t_0) \times 86,400\,\mathrm{s}$$

with

$$L_\mathrm{C} = 1.480827 \times 10^{-8}.$$

Some of the best solar system ephemerides, the DE ephemerides of the Jet Propulsion Laboratory (JPL), do not employ TCB as basic time variable. The original idea was to use a timescale that differs from TT practically only by periodic terms. Strictly speaking, because of arbitrarily long periods contained in the motion of the solar system, such a timescale cannot be realized with ultimate precision. Consequently, the timescales $\mathrm{T_{eph}}$ used in barycentric ephemerides show a relation with TCB or TCG depending slightly upon the ephemeris itself. In the past the DE ephemerides used the Fairhead–Bretagnon series (Fairhead and Bretagnon 1990) to derive $\mathrm{T_{eph}}$ from TT. Meanwhile another barycentric timescale called TDB has been defined by

$$\mathrm{TDB} = \mathrm{TCB} - L_\mathrm{B} \times (\mathrm{JD_{TCB}} - T_0) \times 86,400\,\mathrm{s} + \mathrm{TDB_0}, \tag{2.42}$$

with $T_0 = \mathrm{JD}\,2443144.5003725$,

$$L_\mathrm{B} = 1.550519768 \cdot 10^{-8}, \qquad \mathrm{TDB_0} = -6.55 \times 10^{-5}\,\mathrm{s}\,.$$

The value for L_B was chosen so to minimize the linear drift between TDB and TT for the ephemeris DE405. On the surface of the Earth, this difference is less than 2 ms for the forthcoming centuries.

In the planetary ephemerides developed at Paris Observatory, as described in Fienga et al. (2009), TDB is used for the description of planetary motion, and the differences between TT and TDB are estimated by solving (2.41) at the geocenter at each step of the integration. By using the INPOP values for TT–TDB in the data analysis and the fit of the planetary ephemerides, there is a complete consistency between the positions and velocities of the planets and TT–TDB, all provided to users since INPOP08.

2.16 Fairhead–Bretagnon Series

Analytical approximations for $\Delta T \equiv \mathrm{T_{eph}} - \mathrm{TT}$ are based upon (semi)analytical ephemerides of the solar system. The Fairhead–Bretagnon approximation is based upon the planetary theory VSOP82 (Bretagnon 1982) and the lunar theory ELP2000 (Chapront-Touzé and Chapront 1983). This series is written in the form

$$\begin{aligned}\Delta T = {} & C_0 \mathrm{TT}^2 \\ & + \sum_i A_i \sin(\omega_{ai}\mathrm{TT} + \phi_{ai}) + \mathrm{TT} \sum_i B_i \sin(\omega_{bi}\mathrm{TT} + \phi_{bi}) \\ & + \mathrm{TT}^2 \sum_i C_i \sin(\omega_{ci}\mathrm{TT} + \phi_{ci}) + \mathrm{TT}^3 \sum_i D_i \sin(\omega_{di}\mathrm{TT} + \phi_{di}).\end{aligned} \tag{2.43}$$

Here, TT is counted in millennia since J2000.0 and $\Delta T \equiv \mathrm{T_{eph}} - \mathrm{TT}$ is in microseconds. The first ten coefficients are given in Table 2.2. The full set of 127 coefficients can be found in Fairhead and Bretagnon (1990).

Table 2.2 The ten largest terms in the Fairhead–Bretagnon series for ΔT

i	A_i (μs)	ω_{ai} (rad/1,000 year)	ϕ_{ai} (rad)	Period (year)
1	1656.674564	6283.075943033	6.240054195	1.0000
2	22.417471	5753.384970095	4.296977442	1.0921
3	13.839792	12566.151886066	6.196904410	0.5000
4	4.770086	529.690965095	0.444401603	11.8620
5	4.676740	6069.776754553	4.021195093	1.0352
6	2.256707	213.299095438	5.543113262	29.4572
7	1.694205	−3.523118349	5.025132748	1783.4159
8	1.554905	77713.772618729	5.198467090	0.0809
9	1.276839	7860.419392439	5.988822341	0.7993
10	1.193379	5223.693919802	3.649823730	1.2028

The *AstroRef* package supplies the function `TephOffset` which may be used to calculate ΔT.

2.17 Problems of Time Dissemination

In earlier days sometimes clocks were synchronized by means of clock transport. This, however, is a laborious method that has been ousted by the transmission of electromagnetic signals.

A simple method of time dissemination is the continuous emission of time signals by certain broadcasting stations. In Europe we face four of such stations emitting time signals in the range from 50 to 77.5 kHz. These are the stations: DCF 77 (Mainflingen, Germany), HBG 75 (Prangins, Switzerland), MSF 60 (Rugby, United Kingdom), and OMA 50 (Podebrady, Prague, Czech Republic). From the German *Physikalisch Technische Bundesanstalt* (PTB), Brunswick, via the broadcasting station DCF 77, time signals related with CET are emitted that can be received up to a distance of about 2,000 km. PTB is responsible for the generation of the time signals, whereas *Deutsche Telekom* is responsible for the handling of the antenna arrangements. As emitting antennas vertical 50-kW omnidirectional antennas with a height of 150 or 200 m are in use. The DCF 77 signals at the location of emission (Mainflingen near Frankfurt/M.) are derived from atomic clocks at PTB and are controlled by PTB. The carrier frequency of 77.5 kHz presents a highly stable normal frequency. Not only the second pulses can be used for time dissemination but also the phase leading to a synchronization accuracy of some microseconds.

At this place we would like to mention the navigation system LORAN-C (Long Range Navigation) that mainly served for the position determination of ships and to some extent also of airplanes. It presents an advancement of LORAN-A that was established by MIT during the Second World War. LORAN-C was reconstructed by

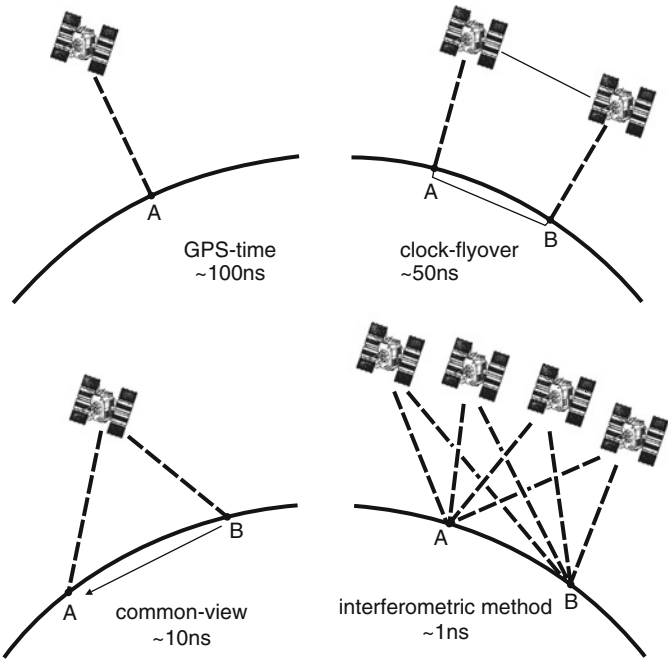

Fig. 2.27 Different methods of time dissemination with GPS

the US Coast Guard almost worldwide and served military as well as civil purposes. For a long time, it was the standard procedure of worldwide time comparisons with an accuracy of about a microsecond. Meanwhile LORAN-C was replaced by GPS as far as possible.

Finally, it should be noted here that in some cases, primary frequency standards are compared by the help of transportable cesium fountains like LNE-SYRTE-FOM.

2.18 Time Dissemination by Means of Satellites

With the adoption of artificial satellites new possibilities opened for the purposes of time dissemination with higher accuracies, larger operating distances, and faster availability. Among the satellite techniques we distinguish one-way and two-way methods. In the active one-way method one uses the time signals of the highly stable onboard clock. If the satellite orbit is known exactly, the signal propagation time to the ground station can be calculated, and the satellite time can be compared with that of the station clock. Uncertainties result from the lack of very precise orbital data, the stability of the satellite clock, and problems with atmospheric refraction. In the passive one-way method, time signals from some master clock on the ground

are emitted to the satellite that merely distributes the information. With the two-way methods time comparisons are accomplished between two station clocks by means of satellites. In this case the satellite has to be equipped with a corresponding transponder that instantaneously reflects the signal.

Of ever increasing prominence is the time dissemination with GPS. With GPS time can be disseminated practically worldwide with an accuracy of about a nanosecond. One distinguishes different methods of time comparisons with GPS (Fig. 2.27):

- Measuring a GPS satellite during a flyover to the ground station and comparison of the ground clock with GPS system time (± 100 ns).
- Flyover a GPS satellite over two ground stations (A and B) and exchange of the measuring results for the determination of the time difference between the clocks at A and B (± 50 ns).
- Simultaneous measurement of a GPS satellite from two ground stations A and B ("common view") and exchange of the measuring results (± 10 ns) and
- simultaneous measurements of several GPS satellites from two ground stations and correlation of signals ("interferometric method"; ± 1 ns).

http://www.springer.com/978-3-642-30225-1

Space-Time Reference Systems
Soffel, M.; Langhans, R.
2013, XIV, 314 p., Hardcover
ISBN: 978-3-642-30225-1